

NONLINEAR SIMULATIONS OF THE HEAT FLUX DRIVEN BUOYANCY INSTABILITY AND ITS IMPLICATIONS FOR GALAXY CLUSTERS

IAN J. PARRISH^{1, 2} AND ELIOT QUATAERT¹*Draft version November 2, 2018***ABSTRACT**

In low collisionality plasmas heat flows almost exclusively along magnetic field lines, and the condition for stability to convection is modified from the standard Schwarzschild criterion. We present local two and three-dimensional simulations of a new heat flux driven buoyancy instability (the HBI) that occurs when the temperature in a plasma decreases in the direction of gravity. We find that the HBI drives a convective dynamo that amplifies an initially weak magnetic field by a factor of ~ 20 . In simulations that begin with the magnetic field aligned with the temperature gradient, the HBI saturates by rearranging the magnetic field lines to be almost purely perpendicular to the initial temperature gradient. This magnetic field reorientation results in a net heat flux through the plasma that is less than 1% of the field-free (Spitzer) value. We show that the HBI is likely to be present in the cool cores of clusters of galaxies between $\sim 0.1 - 100$ kpc, where the temperature increases outwards. The saturated state of the HBI suggests that inward thermal conduction from large radii in clusters is unlikely to solve the cooling flow problem. Finally, we also suggest that the HBI may contribute to suppressing conduction across cold fronts in galaxy clusters.

Subject headings: convection — instabilities — MHD — galaxies: clusters — plasmas

1. INTRODUCTION

For thermally stratified fluids, stability to convection is guaranteed if the entropy decreases in the direction of gravity. In dilute astrophysical plasmas, however, the mean free path is large compared to the gyroradius, and heat conduction is anisotropic with respect to the magnetic field (Braginskii 1965). In the low collisionality regime, the convective instability condition is modified, and plasmas in which the temperature increases in the direction of gravity are buoyantly unstable (Balbus 2000). This instability, called the magnetothermal instability (MTI), has been simulated in two and three dimensions by Parrish & Stone (2005, 2007).

In this *Letter*, we study a related instability of low collisionality plasmas. Quataert (2007) has shown that, in the presence of a background heat flux, anisotropic conduction drives a buoyancy instability when the temperature decreases in the direction of gravity. The growth rates of this heat flux driven buoyancy instability (HBI) are verified using two-dimensional (2D) simulations in §2. In §3 we determine the nonlinear saturation of the HBI in three dimensions (3D) and show that it drives a magnetic dynamo while greatly suppressing the net heat flux through the plasma. Finally, in §4 we apply the HBI to the intracluster medium and discuss its implications for cooling flows and cold fronts.

2. 2D SIMULATIONS**2.1. Equations and Method**

We solve the usual equations of magnetohydrodynamics (MHD) with the addition of anisotropic thermal con-

duction. The MHD equations in conservative form are

$$\frac{\partial \rho}{\partial t} + \nabla \cdot (\rho \mathbf{v}) = 0, \quad (1)$$

$$\frac{\partial (\rho \mathbf{v})}{\partial t} + \nabla \cdot \left[\rho \mathbf{v} \mathbf{v} + \left(p + \frac{B^2}{8\pi} \right) \mathbf{I} - \frac{\mathbf{B} \mathbf{B}}{4\pi} \right] + \rho \mathbf{g} = 0, \quad (2)$$

$$\frac{\partial E}{\partial t} + \nabla \cdot \left[\mathbf{v} \left(E + p + \frac{B^2}{8\pi} \right) - \frac{\mathbf{B} (\mathbf{B} \cdot \mathbf{v})}{4\pi} \right] + \nabla \cdot \mathbf{Q} + \rho \mathbf{g} \cdot \mathbf{v} = 0, \quad (3)$$

$$\frac{\partial \mathbf{B}}{\partial t} + \nabla \times (\mathbf{v} \times \mathbf{B}) = 0, \quad (4)$$

where the symbols have their usual meaning. The total energy E is given by

$$E = \epsilon + \rho \frac{\mathbf{v} \cdot \mathbf{v}}{2} + \frac{\mathbf{B} \cdot \mathbf{B}}{8\pi}, \quad (5)$$

where $\epsilon = p/(\gamma - 1)$. Throughout this paper, we assume $\gamma = 5/3$. The anisotropic electron heat flux is given by

$$\mathbf{Q} = -\chi_C \hat{\mathbf{b}} \hat{\mathbf{b}} \cdot \nabla T, \quad (6)$$

where χ_C is the Spitzer conductivity (Spitzer 1962) and $\hat{\mathbf{b}}$ is a unit vector in the direction of the magnetic field.

We follow the HBI into the nonlinear regime using the conservative MHD code Athena (Gardiner & Stone 2005) with the addition of anisotropic conduction along magnetic field lines as described in Parrish & Stone (2005). This methodology has been extensively utilized and tested previously in the study of the MTI. In all simulations, $g = 1$. The 2D simulations use a linear temperature gradient with fixed temperature boundary conditions at the top and bottom of the domain.

¹ Astronomy Department & Theoretical Astrophysics Center, 601 Campbell Hall, The University of California, Berkeley, CA 94720; iparrish@astro.berkeley.edu; eliot@astro.berkeley.edu

² Chandra Fellow

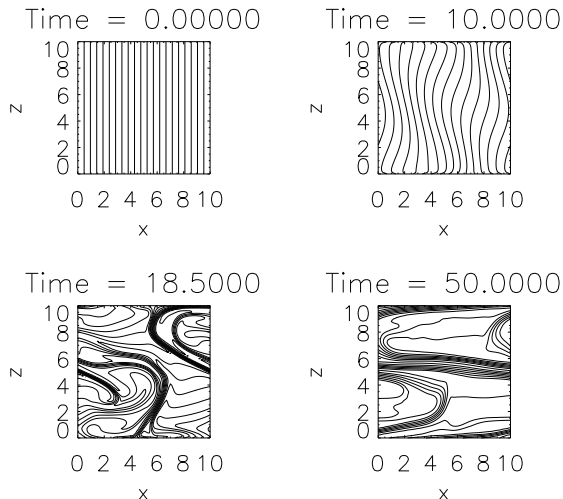


FIG. 1.— Snapshots of the magnetic field in a 2D simulation initialized with a single mode perturbation having $k_x = k_y$. The HBI drives the initially vertical field to become largely horizontal. The units of time in Figs. 1-4 are such that the dynamical time $(g d \ln T / dz)^{-1/2} \approx 1.4$.

2.2. Physics of the HBI

The physical origin of the HBI can best be understood by examining magnetic field snapshots from a 2D simulation, as shown in Figure 1 (see also Fig. 1 of Quataert 2007). This 2D simulation was run at a resolution of $(100)^2$. The initial temperature profile was $T(z) = T_0(1 + z/2)$, the temperature scale-height at the midplane is 2, and the size of the domain is $(0.1)^2$; note that the simulations are local. The pressure and density were chosen so that the atmosphere was in hydrostatic equilibrium with $p \sim \rho \sim 1$. The magnetic field is chosen to be weak initially and purely vertical with $B_0 / (4\pi)^{1/2} = 5 \times 10^{-4}$, so that magnetic tension forces are negligible. The purely anisotropic thermal diffusivity is $\kappa = \chi_C T / P = 10^{-2}$, where κ has units of a diffusion coefficient, i.e., $\text{cm}^2 \text{s}^{-1}$. With these parameters, the conduction time for small-scale perturbations is much less than the dynamical time, which is the limit of fastest growth for the HBI (and MTI).

Figure 1 shows that perturbations with non-zero k_x and k_y generate converging and diverging field lines. The heat flux follows these field lines leading to (conductive) heating and cooling of the plasma. In a plasma with $dT/dz > 0$, a fluid element displaced upwards is thus heated by the background heat flux, causing it to rise further and become buoyant. Note that the magnetic field snapshots in Figure 1 look very similar to snapshots for the MTI rotated by 90° .

For a weak vertical magnetic field, the growth rate of the HBI in the limit of rapid conduction is

$$\omega^2 \approx -g \left(\frac{d \ln T}{dz} \right) \frac{k_\perp^2}{k^2}. \quad (7)$$

For the parameters of our simulation, we predict a growth rate of 0.5 for $k_x = k_y$. Measurement of the growth rate in our single mode simulation verifies this prediction to within 1%. In the 2D simulation, we find that the magnetic energy is amplified by a factor of ~ 52 during

the course of the run. We defer a detailed discussion of the nonlinear saturation to the 3D simulation.

3. NONLINEAR SATURATION IN 3D

Only in 3D can we accurately explore the saturation of the HBI since the nature of convection differs significantly in 2D and 3D and the anti-dynamo theorem applies in 2D (Cowling 1934). Using 3D simulations, we now quantify the amplification of the magnetic field by the HBI and the resulting heat flux through the plasma.

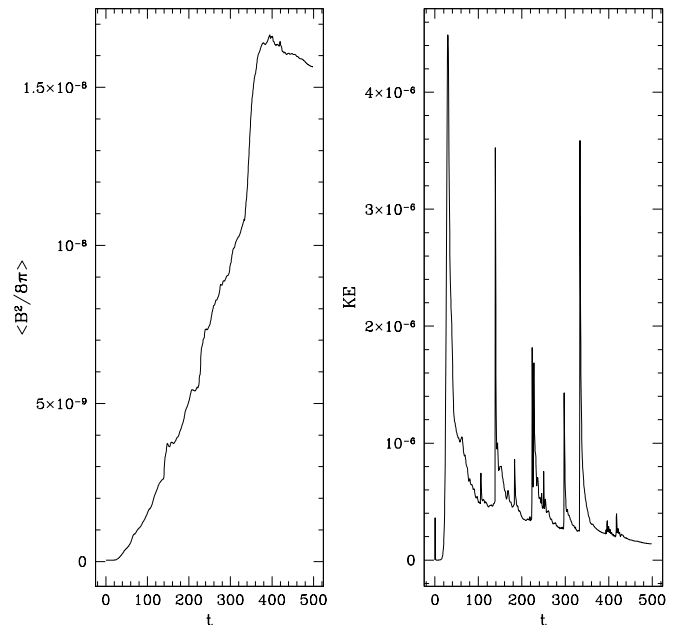


FIG. 2.— Time evolution of the volume-averaged magnetic energy density and kinetic energy density in the HBI-unstable region of run R1. The magnetic energy is amplified by a factor of ~ 300 and is in rough equipartition with the subsonic convective motions.

The computational set-up we use is nearly identical to the stratified box presented in §2.3 of Parrish & Stone (2007); we refer the reader there for details. The box consists of three vertical layers of equal size in which the central region has a linear temperature profile with $\partial T / \partial z > 0$ and pure anisotropic conduction along magnetic field lines, such that it is unstable to the HBI. The top and bottom layers are isothermal atmospheres (exponential pressure and density profiles) and act as a buffer to the penetrative convection that takes place. These regions have isotropic conductivity and are stable to the HBI. For all of the simulations in this paper, the isotropic conductivity in the top and bottom layers is equal to the parallel anisotropic conductivity in the middle region. It is important to note that our box size is again small compared to the temperature scale height (0.2 and 2, respectively), so that our simulations are local in nature. Table 1 gives the initial magnetic field and conductivity for our 3D runs; we will primarily focus on R1, our fiducial simulation.

Figure 2 shows the amplification of magnetic energy as a function of time for R1. The net amplification can be defined by

$$\Delta \langle B^2 \rangle \equiv \frac{\langle B^2 \rangle_{\text{fin}}}{\langle B^2 \rangle_{\text{init}}}, \quad (8)$$

TABLE 1
TABLE OF NONLINEAR RUNS

Run	$B_0/(4\pi)^{1/2}$	κ_{\parallel}	$\Delta\langle B^2 \rangle$	RMS Mach	$\langle \theta_B \rangle$	$f = Q/\tilde{Q}$
R1.....	10^{-5}	5×10^{-3}	327	5.1×10^{-4}	5.8°	0.51%
R2.....	10^{-4}	5×10^{-3}	36.4	7.7×10^{-4}	17.2°	7.7%
R3.....	10^{-5}	1.5×10^{-2}	384	5.1×10^{-4}	3.8°	0.31%

which for the fiducial case is $\Delta\langle B^2 \rangle \sim 327$. In addition to amplifying the field, the HBI drives vertical convective motions. These remain subsonic with an RMS Mach number of 5.1×10^{-4} ; the kinetic energy is ~ 10 times the magnetic energy at the end of R1.

The evolution of the average angle of the magnetic field with respect to the horizontal in the unstable layer is particularly interesting; this is defined by

$$\langle \theta_B \rangle \equiv \left\langle \sin^{-1} \left(\frac{|B_z|}{|B|} \right) \right\rangle. \quad (9)$$

Figure 3 shows $\langle \theta_B \rangle$ for run R1. The buoyant motions

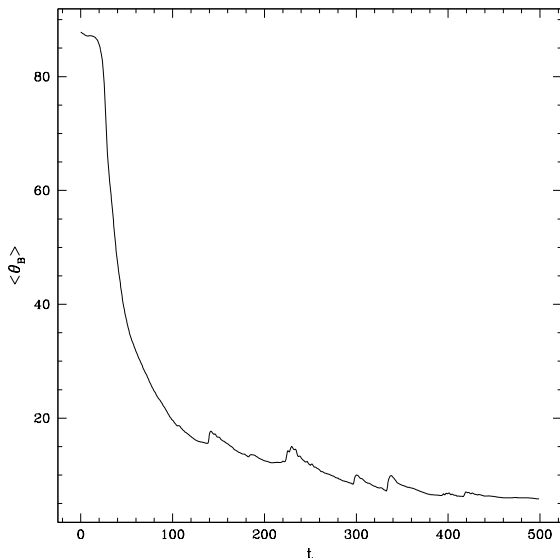


FIG. 3.— Evolution of the average angle of the magnetic field with respect to the horizontal for the fiducial simulation R1. The HBI drives the initially vertical field to become almost purely horizontal with an average angle of only 5.8° .

of the HBI saturate by driving the magnetic field to be largely *perpendicular* to the background temperature gradient. This evolution is in stark contrast to the MTI, which preferentially aligns the magnetic field *with* the background temperature gradient. For R1, the magnetic field evolves from an initially vertical field (90°) to a field with an average angle of $\langle \theta_B \rangle \approx 5.8^\circ$. As one might expect, this dramatically decreases the heat flux through the plasma, as is shown explicitly in Figure 4. It is useful to compare the heat flux in the saturated state of the HBI with the heat flux that is present in the initial state,

$$\tilde{Q} = -\kappa_{\parallel} \left(\frac{dT}{dz} \right)_0. \quad (10)$$

As the HBI evolves and the field lines become more horizontal (Fig. 3), the heat flux across the unstable

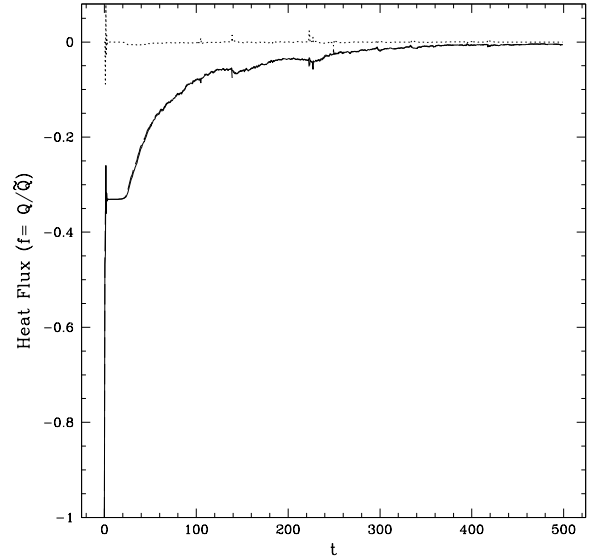


FIG. 4.— Time evolution of the horizontally-averaged vertical heat flux at the midplane in the fiducial simulation R1. The total heat flux (solid line) is divided into the dominant conductive flux (dashed line) and the advective flux (dotted line). Note that the total heat flux and conductive flux are essentially collinear. These fluxes are normalized to the fiducial heat flux, \tilde{Q} , that would be present for vertical magnetic field lines (eq. [10]).

layer plummets. We define the conduction efficiency by $f = Q/\tilde{Q}$. The saturated state of the HBI has a very low heat flux of $f = 5.0 \times 10^{-3}$ for R1; most of this flux is carried by conduction, with only a small contribution from convective motions (Fig. 4). We will discuss the obvious implication of this result for cooling flows shortly.

For a weak initial magnetic field, the saturation of the HBI is primarily due to the reduction in the mean angle of the magnetic field $\langle \theta_B \rangle$. Quataert (2007) showed that for nearly horizontal fields the maximum growth rate of the HBI is given by

$$|\omega| \simeq (g \, d \ln T / dz)^{1/2} \langle \theta_B \rangle. \quad (11)$$

At the conclusion of run R1, the growth rate has decreased by a factor of ~ 10 , to $\omega \simeq 0.07$, significantly reducing the efficacy of the instability. Meanwhile the growth of the magnetic field increases the effects of magnetic tension. The Alfvén frequency (a lengthscale dependent quantity) ranges from 0.01 to 0.7 from the size of the domain down to the grid scale, respectively. Because the Alfvén frequency is comparable to the dynamical frequency on small-scales, and to the growth rate on all but the largest scales, tension will further inhibit the growth of the HBI. Although we cannot rule out modest additional decrease in $\langle \theta_B \rangle$ and the heat flux on timescales

longer than we have simulated, such evolution will take progressively longer as the growth rate decreases further (eq. [11]) and is unlikely to modify the magnetic and kinetic energy, which have saturated (Fig. 2).

For completeness we ran several additional simulations. Run R3 has a conductivity three times higher than the fiducial value. However, since R1 is already in the limit in which the conduction time for small-scale perturbations is rapid compared to the dynamical time, little change is seen from the fiducial simulation. Run R2 has an initial magnetic field one order of magnitude larger than the fiducial run. Due to magnetic tension effects on the scale of this local simulation, R2 saturates earlier and with less magnetic field amplification. The magnetic field is still primarily horizontal upon saturation and the heat flux is strongly suppressed, although by less than in the fiducial simulation. In a global simulation, the saturated state of R2 would be unstable on large-scales, which would lead to additional field amplification and rearrangement.

4. APPLICATIONS AND DISCUSSION

The HBI is predicted to be present from ~ 0.1 –100 kpc in the intracluster medium of galaxy clusters, where the observed temperature increases outwards. For concreteness, consider the cluster A1795 which has an estimated virial mass of $1.2 \times 10^{15} M_{\odot}$ and a scale radius of $r_s = 460$ kpc (Ettori et al. 2002; Zakamska & Narayan 2003). The temperature increases from $\simeq 2$ keV at 10 kpc to $\simeq 7.5$ keV at 100 kpc. Given these parameters, the growth rate of the HBI at $R = 50$ kpc in the limit of weak fields is $\simeq 3 \times 10^{-16} \text{ s}^{-1}$, i.e., a growth time of $\simeq 10^8$ yr. This should be compared to the wavelength(λ)-dependent Alfvén frequency of $\simeq 5 \times 10^{-17} (\lambda/R)^{-1} (B/1\mu\text{G}) \text{ s}^{-1}$ given the measured electron density of $n_e \simeq 0.02 \text{ cm}^{-3}$ at 50 kpc and an assumed $B \sim 1\mu\text{G}$. Thus tension has a small effect for $\lambda \gtrsim 0.1R$. Because the electron mean free path is $\sim 0.05R$, the thermal conductivity is sufficiently high for perturbations to grow on the dynamical time (eq. [7]).

Our simulations presented in §3 were local ($L_z < H$), but their nonlinear outcomes provide a clear lesson for galaxy clusters. So long as magnetic tension is not dominant, the HBI rapidly and efficiently reorients the magnetic field lines to be perpendicular to the background heat flux, resulting in a net heat flux through the plasma that is much less than the field-free Spitzer value. Our results are significantly different from the predictions of Narayan & Medvedev (2001), Chandran & Maron (2004), and Lazarian (2006), all of whom highlight the effects of field line wandering on the effective thermal conductivity of a plasma. Instead, however, our results, and those of Balbus (2000), Parrish & Stone (2007), & Quataert (2007), demon-

strate that the dynamical coupling between anisotropic thermal conduction, the heat flux, and the magnetic field geometry is crucial. For HBI-unstable plasmas, the net result is that heat is transported far less effectively than previously assumed. These conclusions make the cooling flow problem in clusters more severe since the HBI strongly suppresses the transport of energy from the outer parts of clusters ($r > 100$ kpc) to the cooling core. An alternate mechanism is thus necessary to heat the cluster plasma, e.g., feedback from a central AGN. Several additional effects should be accounted for before this conclusion is considered definitively established. First, cosmic rays from a central AGN modify the stability properties of intracluster plasma (Chandran & Dennis 2006). The interplay between the cosmic rays, which tend to drive the system MTI unstable, and the plasma, which by itself is HBI unstable at intermediate radii, may be interesting and complex. In addition, turbulence produced by galactic outflows and galaxy wakes could modify the magnetic field geometry established by the HBI. Finally, given that tension restricts the HBI to scales $\gtrsim 0.1R$, global simulations are clearly required.

An additional potential application of the HBI in clusters is to the suppression of conduction across cold fronts. The canonical cold front is found in the cluster A3667 (Vikhlinin et al. 2001a,b); our numerical values are drawn from this example. The cold front is an abrupt change in plasma properties, with high temperature, low density, low pressure plasma lying outside low temperature, high density, high pressure plasma. The temperature gradient is thus opposite to both the pressure gradient and the cluster’s gravity—an HBI unstable situation. For the gradient scale length, we take the 5 kpc upper limit from *Chandra* measurements and estimate an HBI growth rate of $\omega \approx 3.8 \times 10^{-15} \text{ s}^{-1}$, corresponding to a growth time of 8.5 Myr. For a $1 \mu\text{G}$ field, magnetic tension is modest for perturbations with wavelengths of 5 kpc, suggesting that the HBI can indeed grow. Although the HBI cannot account for the origin of cold fronts, it may help account for their survival. Namely, the HBI will drive the magnetic field to be horizontal in the cold front, suppressing heat transport across the cold front and thus maintaining the temperature gradient in spite of the nominally short conduction times.

We thank Prateek Sharma for useful conversations. EQ was supported in part by NASA grant NNG06GI68G and the David & Lucile Packard Foundation. IJP is supported by NASA through a Chandra Postdoctoral Fellowship grant PF7-80049 awarded by the Chandra X-Ray Center, which is operated by the Smithsonian Astrophysical Observatory for NASA under contract NAS8-03060.

REFERENCES

- Balbus, S. A. 2000, *ApJ*, 534, 420
 Braginskii, S. I. 1965, in *Reviews of Plasma Physics*, Vol. 1, ed. M. A. Leontovich (New York: Consultants Bureau), 205
 Chandran, B. D., & Dennis, T. J. 2006, *ApJ*, 642, 140
 Chandran, B. D. G., & Maron, J. L. 2004, *ApJ*, 602, 170
 Cowling, T.G. 1934, *MNRAS*, 94, 39
 Ettori, S., et al. 2002, *MNRAS*, 331, 635
 Gardiner, T., & Stone, J. 2005, *J. Comp. Phys.*, 205, 509
 Lazarian, A. 2006, *ApJ*, 645, L25
 Narayan, R. & Medvedev, M. V. 2001, *ApJ*, 562, L129
 Parrish, I. J., & Stone, J. M. 2005, *ApJ*, 633, 334
 Parrish, I. J., & Stone, J. M. 2007, *ApJ*, 664, 135
 Quataert, E. 2007, *ApJ*, Accepted, arXiv:0710.5521
 Spitzer, L. 1962, *Physics of Fully Ionized Gases* (New York: Wiley)
 Vikhlinin, A., Markevitch, M., & Murray, S. S. 2001, *ApJ*, 549, L47
 Vikhlinin, A., Markevitch, M., & Murray, S. S. 2001, *ApJ*, 551, 160
 Zakamska, N. L., & Narayan, R. 2003, *ApJ*582, 162